PAPER • OPEN ACCESS

Modification of Pb quantum well states by the adsorption of organic molecules

View the article online for updates and enhancements.

You may also like

Modification of Pb quantum well states by the adsorption of organic molecules

Benjamin Stadtmüller[1,2], **Lisa Grad**[1,4], **Johannes Seidel**[1], **Florian Haag**[1,2], **Norman Haag**[1], **Mirko Cinchetti**[3] and **Martin Aeschlimann**[1]

[1] Department of Physics and OPTIMAS Research Center, TU Kaiserslautern,
Erwin-Schrödinger-Strasse 46, 67663 Kaiserslautern, Germany
[2] Graduate School of Excellence Materials Science in Mainz, Erwin-Schrödinger-Strasse 46,
67663 Kaiserslautern, Germany
[3] Experimentelle Physik VI, Technische Universität Dortmund, 44221 Dortmund, Germany

E-mail: bstadtmueller@physik.uni-kl.de

CrossMark

Abstract
The successful implementation of nanoscale materials in next generation optoelectronic devices crucially depends on our ability to functionalize and design low dimensional materials according to the desired field of application. Recently, organic adsorbates have revealed an enormous potential to alter the occupied surface band structure of tunable materials by the formation of tailored molecule-surface bonds. Here, we extend this concept of adsorption-induced surface band structure engineering to the unoccupied part of the surface band structure. This is achieved by our comprehensive investigation of the unoccupied band structure of a lead (Pb) monolayer film on the Ag(1 1 1) surface prior and after the adsorption of one monolayer of the aromatic molecule 3,4,9,10-perylene-tetracarboxylic-dianhydride (PTCDA). Using two-photon momentum microscopy, we show that the unoccupied states of the Pb/Ag(1 1 1) bilayer system are dominated by a parabolic quantum well state (QWS) in the center of the surface Brillouin zone with Pb p_z orbital character and a side band with almost linear dispersion showing Pb $p_{x/y}$ orbital character. After the adsorption of PTCDA, the Pb side band remains completely unaffected while the signal of the Pb QWS is fully suppressed. This adsorption induced change in the unoccupied Pb band structure coincides with an interfacial charge transfer from the Pb layer into the PTCDA molecule. We propose that this charge transfer and the correspondingly vertical (partially chemical) interaction across the PTCDA/Pb interface suppresses the existence of the QWS in the Pb layer. Our results hence unveil a new possibility to orbital selectively tune and control the entire surface band structure of low dimensional systems by the adsorption of organic molecules.

Keywords: band structure engineering, metal–organic hybrid interfaces, two-photon momentum microscopy, photoemission tomography

(Some figures may appear in colour only in the online journal)

1. Introduction

One of the most important challenges for next generation optoelectronic and spintronic applications is to reveal novel ways to design the properties of the active functional layers as well as of the interfaces between these layers and metallic contacts. In particular, interfaces between different materials are of utmost importance for the overall device performance as they determine the structural properties of the active layers as well as the charge and spin injection efficiency from the metallic contacts into the active materials. In this context, organic semiconductors have emerged as a highly intriguing class of materials which can be functionalized by chemical

synthesis on a single molecular level. This opens the possibility to design the interactions between the organic materials and metal surfaces and thereby to control the interfacial properties of these so called metal–organic hybrid interfaces or, in case of surfaces with non-trivial spin properties, metal–organic spinterfaces [1].

For this reason, extensive experimental and theoretical efforts were devoted to study prototypical organic molecules containing different functional groups or metallic centers adsorbed in monolayer films on noble metal surfaces [2–11]. This resulted in a comprehensive understanding of metal–organic hybrid systems and paved the way towards controlling the structural and electronic properties of molecular monolayer films on surfaces, for instance by alkali metal doping of organic monolayer films [12–15] or by the formation of heteromolecular systems containing two different types of molecules [16–21]. More recently, it was even demonstrated that the adsorption of organic molecules can lead to a severe modification of the occupied part of the surface band structure of topological insulators or Rashba-type surface alloys [22–26]. In particular, it was shown for a $PbAg_2$ surface alloy that only local σ-like bonds between functional molecular groups and surface atoms are strong enough to alter the surface band structure. These findings open a new possibility to engineer the surface band structure by tailored bonds between functionalized organic molecules and surface atoms.

In this work, we extend this concept of adsorption-induced surface band structure engineering to the unoccupied part of the surface band structure. This is an important step towards the functionalization of the charge and spin carrier dynamics of surfaces which is directly linked to the band structure and band dispersion of the unoccupied states. From the manifold of different materials, metallic bilayer systems consisting of thin metallic films grown on metallic surfaces are ideally suited for our study since they reveal a variety of different surface bands with different orbital character [27–32]. In particular, the spatial confinement of electrons in such metallic monolayer films on fcc(1 1 1) surfaces can lead to the existence of quantum well states (QWSs) in the unoccupied part of the surface band structure.

For our study, we have chosen a monolayer film of lead (Pb) grown on Ag(1 1 1) as model system. The structural properties of this bilayer system have already been characterized by Ast *et al* [33] who demonstrated that Pb monolayer films can be grown in long-range ordered commensurate superstructures on the Ag(1 1 1) surface. The formation of homogeneous high quality monolayer films is an important prerequisite for the subsequent adsorption of organic molecules. As prototypical organic adsorbate, we use the aromatic molecule 3,4,9,10-perylene-tetracarboxylic-dianhydride (PTCDA). This molecule was previously employed to successfully manipulate the geometric and electronic properties of a Rashba-type surface alloy by the formation of local σ-like molecule-surface bonds [25, 34]. Here, we first investigate the band structure of the Pb monolayer structure on the Ag(1 1 1) surface. Using two-photon momentum microscopy (2PMM), we are able to show that the unoccupied band structure of the Pb monolayer film on Ag(1 1 1) consists of an electron-like

QWS with p_z orbital character as well as of an almost linear side band with $p_{x/y}$ orbital character. After the adsorption of one monolayer of PTCDA on the Pb–Ag bilayer system, only the QWS with p_z-orbital character is suppressed while the Pb side band with $p_{x/y}$-character is almost unaffected by the molecular adsorption. The suppression of the QWS band can be directly correlated to an interfacial charge transfer from the metallic bilayer films into the molecular layer and the correspondingly chemical molecule-metal bond between PTCDA and the Pb surface. Our results hence suggest that the adsorption of organic molecules can even lead to an orbital selective manipulation the individual sub bands of metallic thin films by the formation of (at least partial) chemical bonds between the molecule and the surface.

2. Experimental details

2.1. Sample preparation

All experiments and the sample preparations were performed under ultra-high vacuum conditions with base pressure better than 5×10^{-10} mbar. The surface of the (1 1 1)-oriented silver crystal was cleaned by repeated cycles of argon ion bombardment and subsequent annealing at a temperature of $T_{sample} = 730$ K. The quality of the Ag(1 1 1) surface was verified by measuring the surface state at the $\bar{\Gamma}$-point of the surface Brillouin zone (SBZ) as well as by the low surface defect density monitored by photoemission electron microscopy. The PTCDA monolayer film on the Pb–Ag bilayer system was prepared in two subsequent steps. First, more than one monolayer of Pb was deposited onto the clean Ag(1 1 1) surface at room temperature. Subsequent sample annealing at $T_{sample} = 450$ K leads to a desorption of Pb atoms from the second Pb layer and to the formation of a homogeneous well-ordered Pb monolayer film on Ag(1 1 1). The success of the sample preparation was confirmed by low energy electron diffraction and momentum resolved photoelectron spectroscopy. The PTCDA monolayer film was subsequently deposited onto the annealed Pb monolayer film at room temperature. The molecular coverage was controlled by the evaporation time and molecular flux of the evaporator. Both parameters were calibrated beforehand using the monolayer structure of PTCDA/Ag(1 1 1) as a reference.

2.2. Momentum microscopy

The momentum resolved photoemission experiments were performed with a momentum microscopy system with dispersive energy filter, i.e. with a photoemission electron microscope operated in k-space mode [35–37]. This photoemission detector allows us to record the complete angular (momentum) distribution of the photoelectrons above the surface as a function of their kinetic energy in a fixed experimental geometry. The occupied valence band structure was recorded with the He–I emission line of a non-monochromatized helium discharge source with an angle of incidence of $65°$ with respect to the sample surface normal. For the 2PMM experiments, we used the second harmonic (SHG, $\hbar\omega = 3.1$ eV) of a
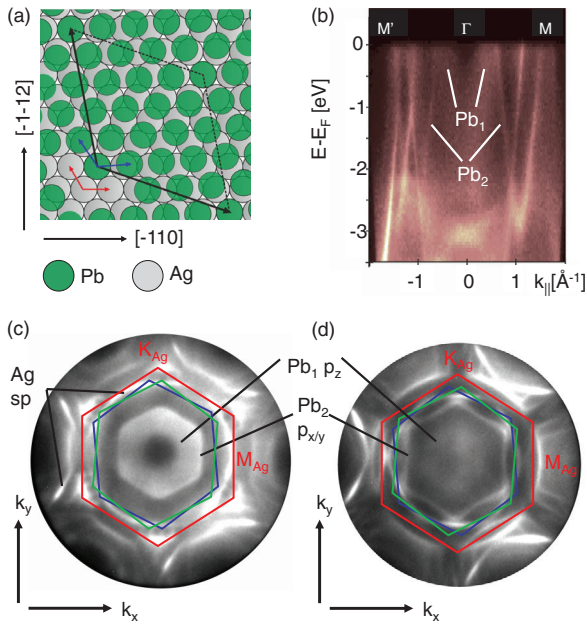
Figure 1. (a) Structural model of the lateral order of the Pb monolayer film on the Ag(1 1 1) surface adapted from the experimental results of [33]. The Ag atoms of the substrate surface are shown as gray balls, the Pb atoms as green balls. The unit cell of the commensurate Pb/Ag superstructure is marked by black arrows, the one of the primitive Ag(1 1 1) and Pb superstructure by red and blue arrows, respectively. Momentum resolved photoemission data of the Pb monolayer film are shown in panels (b)–(d). A band structure cut along the $\overline{\text{M}}' \, \overline{\Gamma} \, \overline{\text{M}}$-high symmetry direction is displayed in (b), a Fermi surface map in (c) and a constant energy map at $E - E_{\text{F}} = -1.4$ eV ($E_{\text{B}} = 1.4$ eV) in panel (d). In both momentum maps, the surface Brillouin zone of Ag(1 1 1) is included as red hexagon, the ones of the mirror domains of the Pb monolayer film as blue and green hexagons.

commercial titanium sapphire laser oscillator system with a pulse width of 30 fs of the SHG radiation and a repetition rate of 80 MHz. The light polarization of the SHG radiation was changed between *s* and *p* using a $\lambda/2$ wave plate. All experiments were performed at room temperature.

3. Results

We start our discussion with the characterization of the geometric and electronic properties of the Pb monolayer film on Ag(1 1 1). The lateral and vertical order of this metallic bilayer system was already characterized by Ast *et al* [33] and their results are summarized in the structural model in figure 1(a). In this model, the Pb atoms are shown in green, the Ag substrate atoms in gray. In the monolayer film, all Pb atoms adsorb on top of the Ag(1 1 1) surface and do not penetrate into the Ag(1 1 1) surface, i.e. they do not form a PbAg$_2$ surface alloy underneath the Pb monolayer film [33, 38]. Most importantly, the vertical corrugation of the Pb film is smaller than 0.09 Å pointing to a very homogeneous morphology of the Pb monolayer film. The lateral arrangement of the Pb atoms can be described by a long range ordered hexagonal superstructure (marked with black arrows in figure 1(a)) on the Ag(1 1 1) surface with the commensurate superstructure

matrix (4, −2;2,6). Most interestingly, the atomic rows of the Pb superstructure are rotated by 4.5° with respect to those of the Ag surface atoms leading to the formation of two symmetry equivalent mirror domains.

In addition, first band structure investigations of the Pb monolayer structure on the Ag(1 1 1) surface have also been conducted previously by Ast *et al* [33] but only along one high symmetry direction of the SBZ, i.e. along the $\overline{\Gamma} \, \overline{\text{K}}$-direction of the Ag SBZ. Ast *et al* were able to identify two sets of Pb derived bands with different orbital character (the corresponding photoemission data are not shown here). The band structure in the center of the SBZ is dominated by an electron-like-band with a large homogeneous linewidth Γ while two additional bands with rather small homogeneous linewidth Γ were observed close to the edge of the SBZ. The orbital character of these different Pb derived bands was obtained in conjunction with a tight binding calculation of a free Pb layer. While the bands with small linewidth were assigned to bands of the free-standing Pb layer with $p_{x/y}$ orbital character, the broad band in the center of the SBZ was attributed to p_z-orbitals of Pb. Thereby, the linewidth broadening was taken as a sign for a hybridization of the p_z-like orbitals of Pb with sp states of the Ag(1 1 1) surface.

In order to obtain a complete picture of the valence band structure of the Pb monolayer film on Ag(1 1 1), we recorded additional momentum microscopy data of the valence band structure throughout the entire SBZ. The yet unexplored band structure along the $\overline{\text{M}}' \, \overline{\Gamma} \, \overline{\text{M}}$-high symmetry direction of the substrate SBZ is shown in figure 1(b). In the following, all high symmetry directions will be refereed to the SBZ of the Ag(1 1 1) substrate. In addition, the Fermi surface as well as a constant energy (CE) map at $E - E_{\text{F}} = -1.4$ eV ($E_{\text{B}} = 1.4$ eV) are included in figures 1(c) and (d). In both CE maps, the SBZ of the primitive unit cells of both rotated Pb domains are shown as blue and green hexagons, the SBZ of the Ag(1 1 1) surface as red hexagon. Upon the adsorption of Pb, the Shockley surface state of the Ag(1 1 1) surface vanishes and is replaced by a set of two new bands with distinct dispersion along the $\overline{\text{M}}' \, \overline{\Gamma} \, \overline{\text{M}}$-direction labeled as Pb$_1$ and Pb$_2$. The band Pb$_1$ is located in the center of the SBZ, Pb$_2$ can only be observed for larger momenta between 0.8 and 1.5 Å^{-1}. All other features can be attributed to the sp-bands of the Ag(1 1 1) surface. Besides the different band dispersion, the most striking difference between Pb$_1$ and Pb$_2$ is the significantly different linewidth Γ of both bands. While the linewidth of Pb$_2$ is comparable to the one of the Ag sp-bands, Pb$_1$ reveals a significantly larger linewidth. This is even better visible in the CE maps in figures 1(c) and (d). For both energies, Pb$_1$ only shows an almost homogeneous intensity distribution in the center of the SBZ with no intensity right at the $\overline{\Gamma}$-point. In contrast, Pb$_2$ appears as a well-defined hexagonal emission feature in momentum space which increases its diameter in momentum space with increasing binding energy.

Our experimental findings of the valence band structure of the Pb monolayer film on Ag(1 1 1) are in line with the previous results by Ast *et al* [33]. This does not only confirm the high quality of our ultrathin Pb films on Ag, but also allows us to identify the origin of the experimentally observed band

structure. In analogy to Ast *et al* [33], we assign Pb_2 to a band of the free-standing Pb layer with $p_{x/y}$ orbital character and Pb_1 to a hybrid band formed by a mixture of Pb p_z orbitals and Ag sp-states. In contrast to the results by Ast *et al*, we only observe one Pb-derived band with $p_{x/y}$-orbital character along the $\overline{M}'\,\overline{\Gamma}\,\overline{M}$-direction. However, this observation is most likely an intrinsic effect of the electronic properties of the free-standing Pb layer and caused by the different arrangement of Pb atoms along the crystallographic high-symmetry directions of the Pb monolayer film associated with the $\overline{M}'\,\overline{\Gamma}\,\overline{M}$ and the $\overline{\Gamma}\,\overline{K}$-directions of the Pb SBZ.

We now turn to the unoccupied part of the Pb–Ag band structure which was investigated by 2PMM using a photon energy of 3.1 eV. The two-photon excitation process is illustrated by two sets of blue arrows in the schematic diagram of the surface projected band structure of Ag(1 1 1) [39] in figure 2(a). In this plot, the gray area represent the three-dimensional (3D) valence band continuum of the Ag bulk bands and the white area the L-band gap in the center of the SBZ. The solid orange line indicates the dispersion of the Shockley surface state [40, 41]. Due to the low photon energy, our 2PMM experiment is only able to access the unoccupied bands in the energy and momentum region marked as blue area in figure 2(a).

We start our discussion with the 2PMM data of the Ag(1 1 1) surface which have been recorded as a reference. Figure 2(b) shows a band structure cut though our 3D 2PMM data stack along the $\overline{M}'\,\overline{\Gamma}\,\overline{M}$-high symmetry direction of the Ag SBZ. We observe two spectroscopic signatures with parabolic dispersion despite the existence of the L-band gap in the entire probed energy and momentum region. Hence, both features cannot be assigned to bands of the unoccupied Ag(1 1 1) band structure. Instead, they are attributed either to the Mahan cone formed by a direct (resonant) sp–sp bulk transition [42] or to the occupied part of the Shockley surface state (labeled SS in figure 2(b)) which can be observed in our 2PMM data due to a strongly detuned transition.

The 2PMM signal changes significantly upon the adsorption of the Pb monolayer on Ag(1 1 1). The corresponding 2PMM cut along the $\overline{M}'\,\overline{\Gamma}\,\overline{M}$-direction recorded with p-polarized light is shown in figure 2(c). In analogy with our VUV-photoemission data discussed above, the Shockley surface state of Ag(1 1 1) vanishes upon the adsorption of Pb and is replaced by a set of new Pb-derived bands arising in the L-band gap. The Pb derived band in the center of the SBZ exhibits a parabolic free electron-like dispersion with an effective band mass of $m^* \approx m_e$ and its band bottom at $E - E_F = 2.38$ eV. As we will discuss below, this band can be attributed to a QWS of the Pb layer. At larger momenta, we observe two branches of a Pb derived side band which cross the high energy cutoff (Fermi edge, $E - E_F = 3.1$ eV) at $\approx \pm 0.5$ Å^{-1} and show an almost linear dispersion. In addition, the Mahan cone-like feature of the resonant transition between two Ag sp bulk bands is also still visible in our 2PMM data.

The dispersion of the unoccupied band structure of the Pb–Ag bilayer system is very similar to findings for a Pb monolayer film on Cu(1 1 1) [27]. However, the orbital character of these unoccupied bands has not been investigated
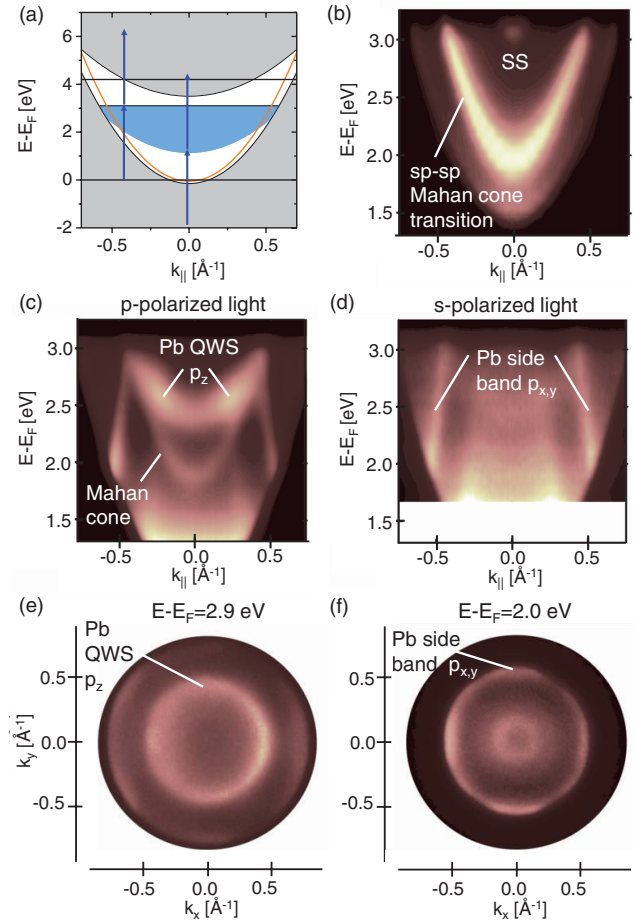

Figure 2. (a) Schematic diagram of the electronic band structure of the Ag(1 1 1) surface. The shaded area represents the three-dimensional (3D) valence band continuum. The orange line represents the 2D Shockley surface state. The two sets of blue arrows illustrate possible two-photon transition and the accessible band structure range of the 2PMM experiment is marked as blue area. Band structure cuts along the $\overline{M}\,\overline{\Gamma}\,\overline{M}$-direction of the Ag SBZ are shown in (b) for the bare Ag(1 1 1) surface, in (c) and (d) for a Pb monolayer film on Ag(1 1 1). All 2PMM data were recorded with a photon energy of $\hbar\omega = 3.1$ eV, the light polarization was varied between p- (panels (b) and (c)) and s-polarized light (d). For the Pb monolayer film, two exemplar CE maps are displayed in (e) and (f) (recorded with p-polarized light).

experimentally so far. Therefore, we repeated our 2PMM experiment with s-polarized light to suppress bands with a strong orbital contribution perpendicular to the surface, i.e. with a strong p_z orbital character. The corresponding band structure cut along the same high-symmetry direction as discussed before is shown in figure 2(d). A direct comparison of the band structure cuts recorded with different light polarizations reveals that the parabolic Pb-derived QWS is only visible for p-polarized excitation. This clearly points to a dominant p_z orbital character of this band. In contrast, both branches of the linear side band can be observed independent of the light polarization which is consistent with an in-plane $p_{x/y}$-like state. This assignment is further supported by the azimuthal intensity distribution of both bands in the CE maps shown in figures 2(e) and (f). The parabolic band around the $\overline{\Gamma}$-point reveals a ring-like shape in figure 2(e) with a homogeneous

azimuthal intensity distribution and hence shows the characteristic emission pattern expected for a free electron-like state. We consequently assign this band to the QWS of the Pb monolayer film, in line with the previous finding of a similar QWS for the Pb–Cu(1 1 1) bilayer system [27]. The linear side band shows a strong azimuthal intensity modulation in figure 2(f). This points to a clear dependency of the electronic properties on the crystallographic in-plane direction of the Pb–Ag bilayer system and consequently to an in-plane character of this band. Accordingly, we attribute the linear side band to $p_{x/y}$-orbitals of the Pb layer. This conclusion is fully supported by tight binding calculations of the Pb–Ag(1 1 1) bilayer system which predict the existence of a Pb $p_{x/y}$ band with a similar band dispersion in the unoccupied part of the Pb–Ag band structure [33] as observed in our 2PMM experiment.

Most interestingly, the spectroscopic signature of the Mahan cone transition of the Pb–Ag bilayer film is also fully suppressed in the 2PMM data recorded with s-polarized light. This is clearly different for the bare Ag(1 1 1) surface, for which the Mahan cone transition between occupied and unoccupied sp bulk bands can be observed independent of the light polarization. This experimental observation strongly suggests a mixing of Pb p_z orbitals with the Ag sp-bands upon the adsorption of Pb on Ag(1 1 1). A similar signature of a strong hybridization between Pb p_z and Ag sp states was also observed in the occupied valence band leading to an unusually broad linewidth of the Pb_1 band in figures 1(b)–(d).

We now turn to the adsorption induced modifications of the unoccupied band structure of the Pb monolayer film on Ag(1 1 1). The band structure of a PTCDA monolayer film on the Pb–Ag(1 1 1) bilayer along the $\overline{M}'\,\overline{\Gamma}\,\overline{M}$-direction is shown in figure 3(a). We find that the Pb derived side bands of $p_{x/y}$ character as well as the Mahan cone feature are still clearly visible even though their intensity is significantly attenuated upon the adsorption of PTCDA. A dedicated analysis allows us to further quantify possible modifications of these spectroscopic features. Both branches of the Pb side band are described by linear functions, the Mahan cone feature by a parabolic curve. The band dispersions resulting from this analysis procedure are shown figure 3(b) as red solid lines together with reference curves extracted from the 2PMM data of the bare Pb monolayer film (shown as blue solid lines in figure 3(b)). Our quantitative analysis reveals an identical dispersion of the Pb side band prior and after the adsorption of one monolayer of PTCDA. This observation is not surprising when considering that the frontier molecular orbitals of π-conjugated adsorbates such as PTCDA preferentially hybridize with surface bands with orbital character perpendicular to the surface. In contrast, the bottom of the Mahan cone parabola shifts 140 meV to higher final state energies. While this shift suggests a modification of the band structure of the Pb–Ag bilayer system, our experimental result cannot be directly correlated to an energy shift of a particular band. The reason for this is that the Mahan cone feature is due to a resonant transition between occupied and unoccupied bands of the Pb–Ag bilayer system. Hence, any change in the energy position of the Mahan cone can
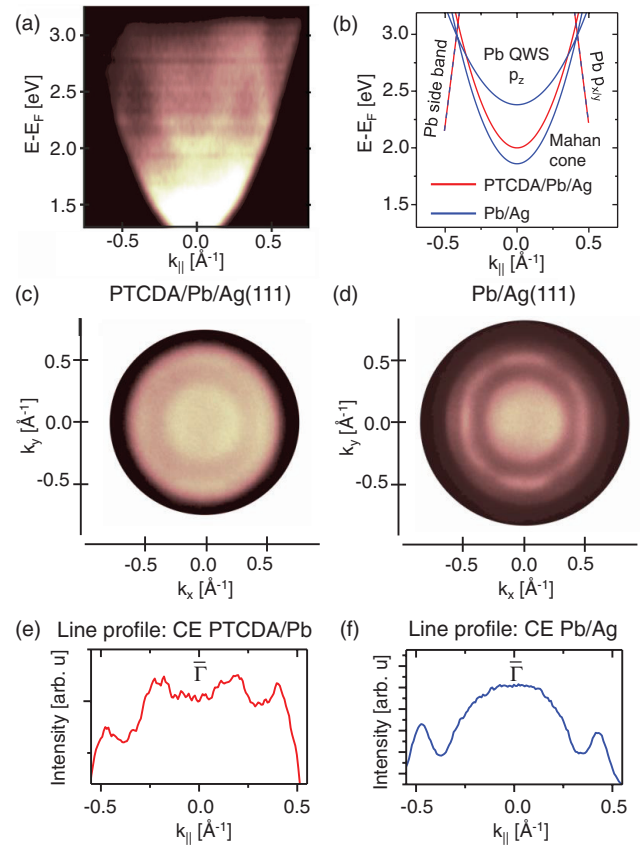

Figure 3. (a) Band structure cut along the $\overline{M}'\,\overline{\Gamma}\,\overline{M}$-direction of a PTCDA monolayer film on the Pb monolayer (p-polarized light). (b) Band dispersion of the Pb side bands as well as of the Mahan cone feature prior (blue solid lines) and after (red solid lines) the adsorption of PTCDA on Pb/Ag(1 1 1). The band dispersions were extracted from the 2PMM data. (c) CE map of the PTCDA/Pb interface at $E - E_F = 2.5$ eV recorded with p-polarized light. The corresponding CE map of the Pb monolayer film is shown in (d) for comparison. Additional radial intensity profiles extracted from both CE maps along a high symmetry direction are displayed in (e) for PTCDA/Pb/Ag(1 1 1) and in (f) for Pb/Ag(1 1 1).

either be caused by a change in the binding energy position of the initial or the final state of this direct transition.

The most severe modification of the unoccupied Pb–Ag band structure is the suppression of the parabolic Pb-derived QWS in the center of the SBZ. This band is no longer visible in the band structure cut in figure 3(a) nor in the CE map at $E - E_F = 2.5$ eV in figure 3(c). The corresponding CE map of the bare Pb monolayer film on Ag(1 1 1) is included in figure 3(d) for comparison. The CE map of the pristine Pb monolayer film reveals a disc-like feature in the center of the SBZ which reflects the emission pattern of the band bottom of the parabolic QWS band superimposed with the ring-like emission feature of the Mahan cone. After the adsorption of PTCDA, the ring-like emission of the Mahan cone is still visible in figure 3(c) while the intensity right at the $\overline{\Gamma}$-point is suppressed by the adsorption of PTCDA. This reduction of intensity at the $\overline{\Gamma}$-point can be observed even more clearly in the radial line profiles extracted from the CE maps of the PTCDA monolayer film on Pb/Ag(1 1 1) (figure 3(e)) and of
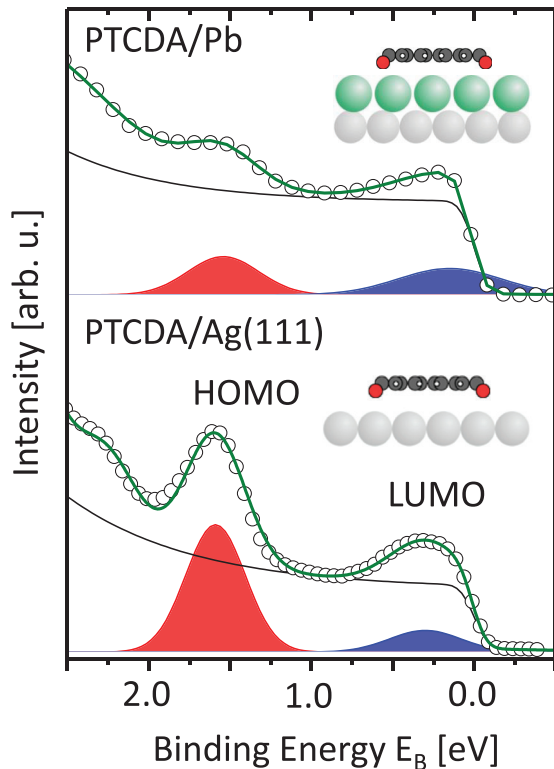
Figure 4. Total photoemission yield of a monolayer film PTCDA on a monolayer Pb on Ag(1 1 1) (upper spectrum) and PTCDA of a monolayer PTCDA adsorbed on the bare Ag(1 1 1) surface (lower spectrum). The experimental data points are shown as circles, the Gaussian functions of our dedicated fitting model as red and blue curve. The envelop of the fitting model is superimposed onto the experimental data as solid green line.

the bare Pb monolayer film on Ag (figure 3(f)). The adsorption of PTCDA results in a clear dip in the otherwise dome-like intensity profile of the CE map of the Pb/Ag(1 1 1) bilayer system right at the $\overline{\Gamma}$-point. All these observations are consistent with an adsorption-induced suppression of the Pb derived QWS state with p_z-orbital character in our 2PMM data.

Our 2PMM data provide conclusive evidence that the interaction between PTCDA and the Pb–Ag(1 1 1) bilayer system is strong enough to alter Pb-derived bands with p_z-orbital character. To gain insight into the mechanism behind the adsorption-induced modification of the unoccupied Pb–Ag(1 1 1) band structure, we now turn to the energy level alignment of the occupied molecular orbitals with respect to the substrate bands. The latter can provide a clear view onto the charge redistribution across the PTCDA-Pb interface. The most essential informations about the energy level alignment can already be deduced from the total photoelectron yield which is shown in the upper panel of figure 4 for a PTCDA monolayer film on the Pb monolayer on Ag(1 1 1). As a reference, a similar spectrum of a PTCDA monolayer film on the bare Ag(1 1 1) surface is included in the lower part of figure 4. At first glance, both photoemission spectra reveal an almost identical line shape. Both spectra exhibit two spectroscopic features at very similar binding energies. For the PTCDA/Ag(1 1 1) interface, the origin of these molecular features has already been extensively investigated both experimentally and

theoretically [2, 43–45]. The maximum at larger binding energies of ≈ 1.6 eV is the spectroscopic signature of the highest occupied molecular orbital (HOMO) while the second feature right at the Fermi energy is derived from the lowest unoccupied molecular orbital (LUMO) of the free molecule. The latter becomes particularly occupied on the Ag(1 1 1) surface due to a (partial) chemical interaction between PTCDA and the surface resulting in an interfacial charge transfer from the surface into the LUMO of PTCDA. For the PTCDA/Pb interface, we hence propose a similar energy level alignment: we assign the spectroscopic feature at larger binding energies ($E_B \approx 1.6$ eV) to the emission signal of the PTCDA HOMO, the one right at the Fermi energy to the one of a LUMO derived state.

Using a dedicated fitting model, we find only marginal quantitative differences between the energy level alignment of the PTCDA/Ag(1 1 1) and of the PTCDA/Pb interface. All molecular features are described by Gaussian functions and the best fitting model is shown in figure 4 underneath the experimental data. The binding energy of the HOMO level (red curve) of the PTCDA/Pb interface is $E_B = 1.54$ eV and hence shifted by 50 meV towards smaller binding energies compared to the PTCDA/Ag(1 1 1) interface. For both adsorbate systems, the spectroscopic LUMO feature is cut by the Fermi edge pointing to a partial charge transfer into the molecule. However, the LUMO binding energy for PTCDA/Pb/Ag(1 1 1) is only $E_B = 0.15$ eV which is 150 meV smaller compared to the reference system PTCDA/Ag(1 1 1). This suggests a weaker charge redistribution between PTCDA and Pb and hence points to a weaker chemical interaction between PTCDA and the Pb layer compared to PTCDA and the Ag(1 1 1) surface.

To further confirm the charge transfer from the Pb monolayer film into the PTCDA LUMO, we now focus on the momentum resolved photoemission yield of the LUMO-derived feature for both adsorbate systems. The recorded CE maps are shown in figure 5(a) for PTCDA/Pb/Ag(1 1 1) and in figure 5(b) for PTCDA/Ag(1 1 1). In both CE maps, the molecular emission features reveal an overall intensity increase from negative to positive momenta (from left to right in figures 5(a) and (b)). This is not an intrinsic feature of the molecular emission pattern, but can be explained by the experimental geometry of the momentum microscopy setup leading to a linear dichroism in the photoemission signal [46]. Apart from this momentum dependent intensity variation, both CE maps exhibit six well defined emission maxima in momentum space which are arranged in a hexagonal pattern around the $\overline{\Gamma}$-point of the SBZ. The width of the momentum space maxima in azimuthal and radial directions are almost identical for both adsorbate systems suggesting indeed that both emission pattern can indeed be assigned to the same molecular orbital, i.e. to the LUMO of PTCDA.

Most interestingly, the hexagonal emission pattern of the PTCDA/Pb interface is rotated by 30° with respect to the one of PTCDA/Ag(1 1 1). This observation strongly suggests a different in-plane (azimuthal) orientation of the PTCDA molecules on both surfaces. Such characteristic differences in the emission pattern can be explained in the framework of photoemission tomography (PT) which
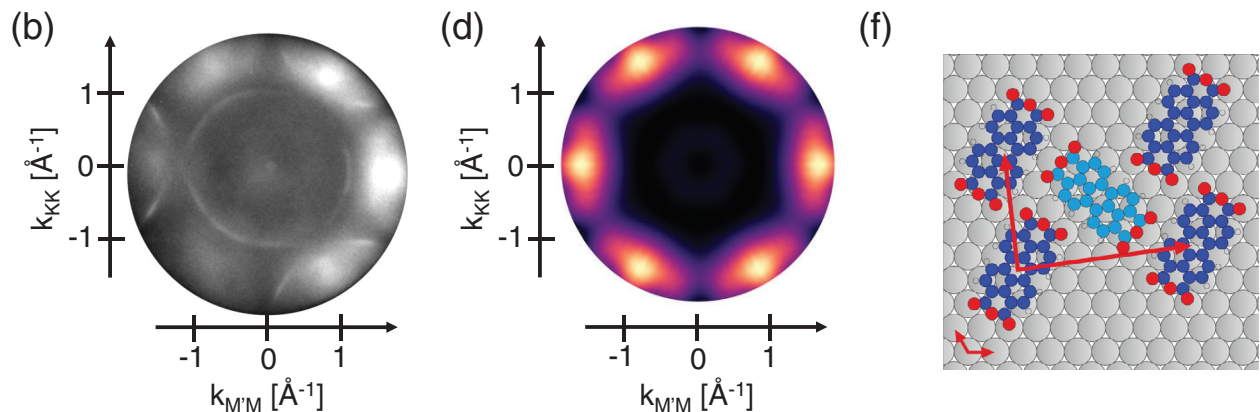
PTCDA/Pb
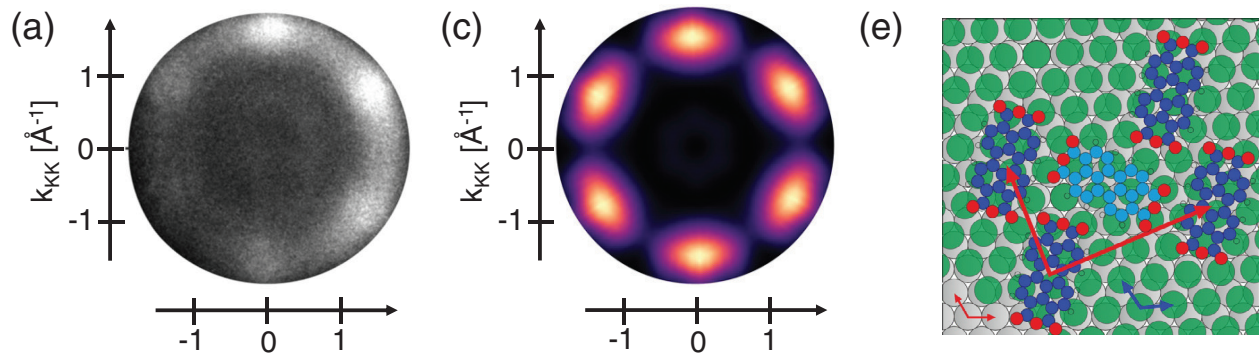
PTCDA/Ag(111)

Figure 5. Momentum resolved photoemission yield of the LUMO feature (blue Gaussian curve in figure 4) is shown in (a) for PTCDA/Pb/Ag(1 1 1) and in (b) for PTCDA/Ag(1 1 1). The theoretical simulations of the momentum space pattern of the LUMO calculated in the framework of photoemission tomography are included in (c) and (d). The simulations are based on density functional theory calculations of a free PTCDA molecule and are symmetrized according to the orientation of the PTCDA molecules on the respective surfaces and the p3m1-symmetry of the Ag(1 1 1) substrate. The corresponding structural model of the PTCDA/Pb/Ag(1 1 1) interface is shown (e), the one of PTCDA/Ag(1 1 1) monolayer film in (f).

allows one to directly correlate the emission pattern of molecular films to the emitting molecular orbitals as well as to the orientation of the molecules on the surface [43, 47, 48]. In the simplest cases, the PT simulations are based on molecular orbital wave functions obtained by density functional theory (DFT) for a single molecule in the gas phase. The simulated emission pattern hence only reflects one single molecular orientation on the surface. For highly symmetric surfaces, however, the azimuthal alignment of all molecule within the unit cell as well as all structurally equivalent orientations due to rotational and mirror domains of the surface have to be considered [43, 49]. Following the established procedure for highly symmetric fcc(1 1 1) surfaces [43], we modeled the characteristic emission pattern of the PTCDA LUMO for both adsorbate systems. The resulting CE maps are shown in figures 5(c) and (d). The PT simulation for PTCDA/Ag(1 1 1) is based on the structural model by Kraft *et al* [44] which is illustrated in figure 5(f). The PTCDA monolayer film reveals two PTCDA molecules per unit cell which are rotated by 60° (molecule A, dark blue circles) and 137° (molecule B, light blue circles) with respect to the [−1 1 0] direction of the Ag(1 1 1) surface. Our simulation hence reveals strong emission maxima along the

$\overline{\Gamma}\ \overline{M}$- direction of the SBZ which perfectly resembles the experimental observation, in analogy with a previous PT study of PTCDA/Ag(1 1 1) [43].

For PTCDA on the Pb–Ag(1 1 1) bilayer, the best agreement between the PT simulation and the momentum resolved photoemission yield was obtained for structural model shown in figure 5(e). This structural arrangement of the PTCDA molecules was obtained by a counter clockwise in-plane rotation of the well-known PTCDA superstructure on Ag(1 1 1) by 15°. The corresponding azimuthal orientation of both structurally inequivalent PTCDA molecules on Pb are 75° and 152° with respect to the [−1 1 0] direction of the Ag(1 1 1) surface for molecule A (dark blue circles) and B (light blue circles), respectively. The different azimuthal orientation of PTCDA on both surfaces is caused by the tendency of elongated molecules to align along high symmetry directions of the substrate. In the case of the Pb/Ag(1 1 1) interface, the hexagonal lattice of the Pb atoms is rotated by 4.5° with respect to the Ag(1 1 1) surface grid. Consequently, our experimental findings suggest that PTCDA forms a herringbone structure on Pb with one molecular species (molecule B, light blue circles) oriented with its long molecular axis perpendicular to rows of Pb surface atoms. Most

importantly, the different orientation of PTCDA on the Pb monolayer and the bare Ag(1 1 1) in conjunction with our PT analysis allows us to unambiguously assign the spectroscopic feature at the Fermi energy of the PTCDA/Ag interface to the LUMO of PTCDA molecules on the Pb monolayer film. This interfacial charge transfer from the Pb layer into PTCDA monolayer film hence points to an at least partial chemical interaction between the PTCDA molecule and the Pb surface. In the following, we will discuss the correlation between this partially chemical interaction and the adsorption induced modification of the Pb QWS.

4. Discussion

Our comprehensive investigation of electronic properties of a Pb monolayer film on Ag(1 1 1) prior and after the adsorption of PTCDA has revealed an intriguing modification of the unoccupied Pb/Ag(1 1 1) band structure upon the adsorption of PTCDA. The unoccupied band structure of the bare Pb monolayer film consists of a linear side-band with in-plane $p_{x/y}$ orbital character as well as a parabolic QWS with p_z orbital character. After the adsorption of a PTCDA monolayer film on the Pb surface, the spectroscopic signal of the Pb QWS is complete suppressed while no change of the band dispersion of the Pb side band with in-plane orbital character can be observed. The modification of the unoccupied Pb/Ag(1 1 1) band structure coincides with an interfacial charge transfer from the Pb surface layer into the LUMO of PTCDA molecules located on the Pb/Ag(1 1 1) bilayer system. This interfacial charge reorganization is a clear fingerprint of an at least partial chemical interaction between the PTCDA layer and the underlying Pb surface. We believe that this (at least partial) chemical interaction is the origin for the adsorption induced suppression of the QWS in the unoccupied part of the Pb/Ag(1 1 1) band structure.

The most straight forward explanation for the suppression of the QWS in our 2PMM data would be an energetic shift of the QWS band due to a direct hybridization of the QWS with molecular orbitals of PTCDA. Energy shifts of surface bands towards the vacuum level energies have already been observed for the Shockley surface state of noble metal surfaces after the adsorption of organic adsorbates [10, 50–52]. These observations revealed a clear trend: the magnitude of the energy shift of these hybrid surface states or *interface states* increases with decreasing bonding distance between the organic adsorbate and the metallic surface [50]. For the PTCDA/Pb/Ag(1 1 1) interface, the vanishing intensity of the QWS could only be expained by an energy shift of at least $\Delta E_{QWS} = 0.72\,\mathrm{eV}$. According to model simulations by Armbrust *et al* [50], such a large energy shift should coincide with a bonding distance of 2.70 ± 0.15 Å between the carbon backbone of PTCDA and the Pb atoms. This bonding distance is significantly smaller than the vertical distance between weakly chemisorbed PTCDA molecules and the Pb atoms of a PbAg$_2$ surface alloy (3.14 ± 0.04 Å determined by the normal incidence x-ray standing waves technique [34]). Hence, we propose that the vanishing intensity of the QWS in our 2PMM experiments is most likely not due to an energy shift of the QWS to larger

intermediate state energies, but caused by a true suppression of the QWS of the Pb layer.

For the pristine Pb monolayer on Ag(1 1 1), the formation of a QWS is due to a confinement of electrons within the Pb layer in the direction perpendicular to the surface [30]. In analogy to the quantum mechanical model system of a particle in a box, the electrons in the Pb layer with energies inside the L- band gap are confined between the vacuum barrier on the vacuum side and the projected bulk band gap of the Ag(1 1 1) crystal on the metal side. Upon the formation of a PTCDA/Pb interface, the interaction and the charge redistribution between PTCDA and the Pb layer results in a severe modification of the potential barrier on the vacuum side. In particular, we suspect that the partial chemical character of the vertical PTCDA-Pb bonding and a corresponding mixing of Pb and PTCDA states lifts the confinement of the former QWS electrons in the Pb layer and is hence responsible for suppression of the QWS of the Pb monolayer film. In contrast, the vertical chemical interaction does not affect the Pb states with an in-plane orbital character. This is mainly due to the low spatial overlap of these Pb derived states with the most frontier orbitals of PTCDA with dominant p_z orbital character. This prevents a direct hybridization between molecular orbitals and in-plane states of Pb. The latter is however required for an adsorption induced manipulation of the surface band structure.

Hence, our results provide evidence that the vertical, partial chemical interaction between the prototypical molecule PTCDA and the Pb monolayer on Ag(1 1 1) is responsible for the orbital selective modification of the unoccupied band structure of the metallic bilayer system. We expect that this phenomena is not exclusive for the Pb/Ag bilayer system but may also occur in other metal–organic hybrid interfaces consisting of organic adsorbates and low dimensional bilayer structures.

5. Summary

In our work, we have studied the unoccupied band structure of a Pb monolayer film on the Ag(1 1 1) structure prior and after the adsorption of the prototypical organic molecule PTCDA by 2PMM with different light polarizations. We find that the unoccupied states of the pristine Pb monolayer film reveal two characteristic Pb derived bands of different orbital character: (i) a parabolic QWS band with p_z orbital character in the center of the SBZ and (ii) a side band at larger momenta with Pb $p_{x/y}$ orbital character. The QWS band is caused by the vertical confinement of electrons in the Pb layer. After the adsorption of PTCDA, we observe characteristic changes in the unoccupied Pb band structure. While the spectroscopic signal of the Pb QWS is fully suppressed by the adsorption of PTCDA, the Pb side band is completely unaffected by the presence of PTCDA. Using linear VUV-photoemission, we find that the modification of the unoccupied Pb states coincides with an interfacial charge transfer from the Pb layer into the LUMO of PTCDA pointing to an at least partial chemical interaction between PTCDA and the Pb layer. We propose that this vertical interaction across the PTCDA/Pb interfaces leads to a mixing of PTCDA orbitals with Pb states. The latter lifts

the confinement of electrons to the Pb layer which, in turn, suppresses the existence of QWS in the Pb layer. This opens the possibility for an orbital selective manipulation of the electronic properties of ultrathin metallic films by the adsorption of organic molecules.

In conclusion, our findings hence clearly show that the established concept of band structure engineering of occupied states by adsorption of organic molecules can be extended to the unoccupied band structure. This opens the possibility to fully control the properties of charge and spin carriers at surfaces by rational design of metal-molecule surface bonding.

Acknowledgments

ORCID iDs

Benjamin Stadtmüller https://orcid.org/0000-0001-8439-434X

References

[1] Cinchetti M, Dediu V A and Hueso L E 2017 Activating the molecular spinterface *Nat. Mater.* **16** 507–15

[2] Duhm S, Gerlach A, Salzmann I, Bröker B, Johnson R L, Schreiber F and Koch N 2008 PTCDA on Au(1 1 1), Ag(1 1 1) and Cu(1 1 1): correlation of interface charge transfer to bonding distance *Org. Electron.* **9** 111–8

[3] Heimel G *et al* 2013 Charged and metallic molecular monolayers through surface-induced aromatic stabilization *Nat. Chem.* **5** 187–94

[4] Romaner L, Heimel G, Brédas J-L, Gerlach A, Schreiber F, Johnson R L, Zegenhagen J, Duhm S, Koch N and Zojer E 2007 Impact of bidirectional charge transfer and molecular distortions on the electronic structure of a metal–organic interface *Phys. Rev. Lett.* **99** 256801

[5] Ruiz V G, Liu W, Zojer E, Scheffler M and Tkatchenko A 2012 Density-functional theory with screened van der Waals interactions for the modeling of hybrid inorganic–organic systems *Phys. Rev. Lett.* **108** 146103

[6] Romaner L, Nabok D, Puschnig P, Zojer E and Ambrosch-Draxl C 2009 Theoretical study of PTCDA adsorbed on the coinage metal surfaces, Ag(1 1 1), Au(1 1 1) and Cu(1 1 1) *New J. Phys.* **11** 053010

[7] Gottfried J M 2015 Surface chemistry of porphyrins and phthalocyanines *Surf. Sci. Rep.* **70** 259–379

[8] Willenbockel M, Lüftner D, Stadtmüller B, Koller G, Kumpf C, Soubatch S, Puschnig P, Ramsey M G and Tautz F S 2015 The interplay between interface structure, energy level alignment and chemical bonding strength at organic-metal interfaces *Phys. Chem. Chem. Phys.* **17** 1530–48

[9] Wiessner M, Ziroff J, Forster F, Arita M, Shimada K, Puschnig P, Schöll A and Reinert F 2013 Substrate-mediated band-dispersion of adsorbate molecular states *Nat. Commun.* **4** 1514

[10] Schwalb C H, Sachs S, Marks M, Schöll A, Reinert F, Umbach E and Höfer U 2008 Electron lifetime in a Shockley-type metal–organic interface state *Phys. Rev. Lett.* **101** 146801

[11] Stadtmüller B, Kröger I, Reinert F and Kumpf C 2011 Submonolayer growth of CuPc on noble metal surfaces *Phys. Rev.* B **83** 085416

[12] Baby A *et al* 2017 Fully atomistic understanding of the electronic and optical properties of a prototypical doped charge-transfer interface *ACS Nano* **11** 10495–508

[13] Mercurio G, Bauer O, Willenbockel M, Fiedler B, Sueyoshi T, Weiss C, Temirov R, Soubatch S, Sokolowski M and Tautz F S 2013 Tuning and probing interfacial bonding channels for a functionalized organic molecule by surface modification *Phys. Rev.* B **87** 121409

[14] Reinisch E M, Ules T, Puschnig P, Berkebile S, Ostler M, Seyller T, Ramsey M G and Koller G 2014 Development and character of gap states on alkali doping of molecular films *New J. Phys.* **16** 023011

[15] Cinchetti M, Neuschwander S, Fischer A, Ruffing A, Mathias S, Wüstenberg J-P and Aeschlimann M 2010 Tailoring the spin functionality of a hybrid metal–organic interface by means of alkali-metal doping *Phys. Rev. Lett.* **104** 217602

[16] Stadtmüller B *et al* 2014 Unexpected interplay of bonding height and energy level alignment at heteromolecular hybrid interfaces *Nat. Commun.* **5** 3685

[17] Stadtmüller B, Schröder S and Kumpf C 2015 Heteromolecular metal–organic interfaces: electronic and structural fingerprints of chemical bonding *J. Electron. Spectrosc. Relat. Phenom.* **204** 80–91

[18] Goiri E, Borghetti P, El-Sayed A, Ortega J E and de Oteyza D G 2016 Multi-component organic layers on metal substrates *Adv. Mater.* **28** 1340–68

[19] Henneke C, Felter J, Schwarz D, Tautz F S and Kumpf C 2017 Controlling the growth of multiple ordered heteromolecular phases by utilizing intermolecular repulsion *Nat. Mater.* **16** 628–33

[20] Cochrane K A, Roussy T S, Yuan B, Tom G, Mårsell E and Burke S A 2018 Molecularly resolved electronic landscapes of differing acceptor–donor interface geometries *J. Phys. Chem. C* **122** 8437–44

[21] Rodríguez-Fernández J *et al* 2017 Tuning intermolecular charge transfer in donor–acceptor two-dimensional crystals on metal surfaces *J. Phys. Chem. C* **121** 23505–10

[22] Jakobs S *et al* 2015 Controlling the spin texture of topological insulators by rational design of organic molecules *Nano Lett.* **15** 6022–9

[23] Caputo M *et al* 2016 Manipulating the topological interface by molecular adsorbates: adsorption of Co-Phthalocyanine on Bi₂Se₃ *Nano Lett.* **16** 3409–14

[24] Wu L, Ireland R M, Salehi M, Cheng B, Koirala N, Oh S, Katz H E and Armitage N P 2016 Tuning and stabilizing topological insulator Bi₂Se₃ in the intrinsic regime by charge extraction with organic overlayers *Appl. Phys. Lett.* **108** 221603

[25] Stadtmüller B *et al* 2016 Modifying the surface of a Rashba-split Pb–Ag alloy using tailored metal–organic bonds *Phys. Rev. Lett.* **117** 096805

[26] Friedrich R, Caciuc V, Zimmermann B, Bihlmayer G, Atodiresei N and Blügel S 2017 Creating anisotropic spin-split surface states in momentum space by molecular adsorption *Phys. Rev.* B **96** 085403

[27] Mathias S, Ruffing A, Deicke F, Wiesenmayer M, Aeschlimann M and Bauer M 2010 Band structure

dependence of hot-electron lifetimes in a Pb/Cu(1 1 1) quantum-well system *Phys. Rev.* B **81** 155429

[28] Becker M and Berndt R 2010 Scattering and lifetime broadening of quantum well states in Pb films on Ag(1 1 1) *Phys. Rev.* B **81** 205438

[29] Ellguth M, Tusche C and Kirschner J 2015 Optical generation of hot spin-polarized electrons from a ferromagnetic two-dimensional electron gas *Phys. Rev. Lett.* **115** 266801

[30] Milun M, Pervan P and Woodruff D P 2002 Quantum well structures in thin metal films: simple model physics in reality? *Rep. Prog. Phys.* **65** 99

[31] Zugarramurdi A, Zabala N, Silkin V M, Chulkov E V and Borisov A G 2012 Quantum-well states with image state character for Pb overlayers on Cu(1 1 1) *Phys. Rev.* B **86** 075434

[32] Mathias S, Wiesenmayer M, Aeschlimann M and Bauer M 2006 Quantum-well wave-function localization and the electron–phonon interaction in thin Ag nanofilms *Phys. Rev. Lett.* **97** 236809

[33] Ast C R, Pacilé D, Papagno M, Gloor T, Mila F, Fedrigo S, Wittich G, Kern K, Brune H and Grioni M 2006 Orbital selective overlayer-substrate hybridization in a Pb monolayer on Ag(1 1 1) *Phys. Rev.* B **73** 245428

[34] Stadtmüller B, Haag N, Seidel J, van Straaten G, Franke M, Kumpf C, Cinchetti M and Aeschlimann M 2016 Adsorption heights and bonding strength of organic molecules on a Pb–Ag surface alloy *Phys. Rev.* B **94** 235436

[35] Krömker B, Escher M, Funnemann D, Hartung D, Engelhard H and Kirschner J 2008 Development of a momentum microscope for time resolved band structure imaging *Rev. Sci. Instrum.* **79** 053702

[36] Tusche C, Krasyuk A and Kirschner J 2015 Spin resolved bandstructure imaging with a high resolution momentum microscope *Ultramicroscopy* **159** 520–9

[37] Yan B, Stadtmüller B, Haag N, Jakobs S, Seidel J, Jungkenn D, Mathias S, Cinchetti M, Aeschlimann M and Felser C 2015 Topological states on the gold surface *Nat. Commun.* **6** 10167

[38] Zhang K H L *et al* 2011 Observation of a surface alloying-to-dealloying transition during growth of Bi on Ag(1 1 1) *Phys. Rev.* B **83** 235418

[39] Canário A R, Kravchuk T and Esaulov V A 2006 Bandgaps, surface states and the anomalous neutralization of Li$^+$ on (1 1 1) surfaces of noble metals *New J. Phys.* **8** 227

[40] Heimann P, Neddermeyer H and Roloff H F 1977 Ultraviolet photoemission for intrinsic surface states of the noble metals *J. Phys. C: Solid State Phys.* **10** L17

[41] Nicolay G, Reinert F, Schmidt S, Ehm D, Steiner P and Hüfner S 2000 Natural linewidth of the Ag(1 1 1) L-gap surface state as determined by photoemission spectroscopy *Phys. Rev.* B **62** 1631

[42] Winkelmann A, Sametoglu V, Zhao J, Kubo A and Petek H 2007 Angle-dependent study of a direct optical transition in the Sp-bands of Ag(1 1 1) by one- and two-photon photoemission *Phys. Rev.* B **76** 195428

[43] Stadtmüller B *et al* 2012 Orbital tomography for highly symmetric adsorbate systems *Europhys. Lett.* **100** 26008

[44] Kraft A, Temirov R, Henze S K M, Soubatch S, Rohlfing M and Tautz F S 2006 Lateral adsorption geometry and site-specific electronic structure of a large organic chemisorbate on a metal surface *Phys. Rev.* B **74** 041402

[45] Zou Y, Kilian L, Schöll A, Schmidt Th, Fink R and Umbach E 2006 Chemical bonding of PTCDA on Ag surfaces and the formation of interface states *Surf. Sci.* **600** 1240–51

[46] Cherepkov N A and Schönhense G 1993 Linear dichroism in photoemission from oriented molecules *Europhys. Lett.* **24** 79

[47] Puschnig P, Berkebile S, Fleming A J, Koller G, Emtsev K, Seyller T, Riley J D, Ambrosch-Draxl C, Netzer F P and Ramsey M G 2009 Reconstruction of molecular orbital densities from photoemission data *Science* **326** 702–6

[48] Willenbockel M *et al* 2013 Energy offsets within a molecular monolayer: the influence of the molecular environment *New J. Phys.* **15** 033017

[49] Feyer V, Graus M, Nigge P, Wießner M, Acres R G, Wiemann C, Schneider C M, Schöll A and Reinert F 2014 Adsorption geometry and electronic structure of iron phthalocyanine on Ag surfaces: a LEED and photoelectron momentum mapping study *Surf. Sci.* **621** 64–8

[50] Armbrust N, Schiller F, Güdde J and Höfer U 2017 Model potential for the description of metal/organic interface states *Sci. Rep.* **7** 46561

[51] Temirov R, Soubatch S, Luican A and Tautz F S 2006 Free-electron-like dispersion in an organic monolayer film on a metal substrate *Nature* **444** 350

[52] Caplins B W, Suich D E, Shearer A J and Harris C B 2014 Metal/phthalocyanine hybrid interface states on Ag(1 1 1) *J. Phys. Chem. Lett.* **5** 1679–84